iScience, Volume *24*

Supplemental information

Microscopy deep learning predicts virus infections and reveals mechanics of lytic-infected cells

Vardan Andriasyan, Artur Yakimovich, Anthony Petkidis, Fanny Georgi, Robert Witte, Daniel Puntener, and Urs F. Greber

Supplemental Data

Suppl. Fig. S1: CNN architecture, dataset generation pipelines and training quality of ViResNet for infection classification (related to Fig. 1).

A) Effect of Hoechst on AdV plaque formation.

B) Training dataset generation pipeline for infection classification.

C) ViResNet architecture schematic.

D) ROC curves for infection prediction (AdV, HSV-1) of trained ViResNet, Decision tree, SVM and k-NN classifiers.

E) ViResNet infection prediction for AdV-C5-IX-FS2A-GFP. Note that AdV-C5 is a distinct serotype from AdV-C2, which was used for network training. The infection prediction for AdV-C5 yielded 93% accuracy.

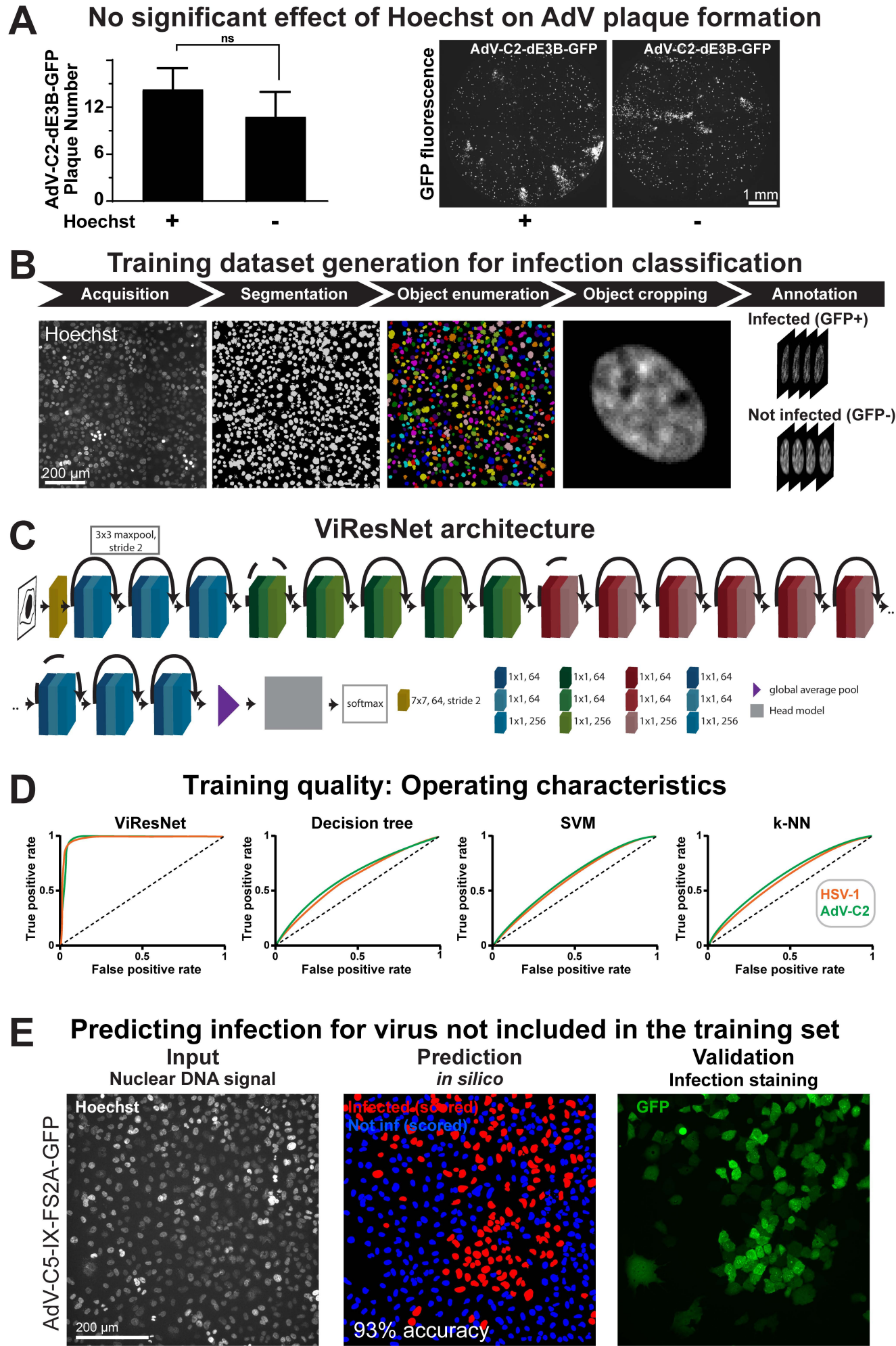
A
No significant effect of Hoechst on AdV plaque formation
ns
AdV-C2-dE3B-GFP Plaque Number
12
6
0
Hoechst
+
-
GFP fluorescence
AdV-C2-dE3B-GFP
AdV-C2-dE3B-GFP
1 mm
+
-
B
Training dataset generation for infection classification
Acquisition
Segmentation
Object enumeration
Object cropping
Annotation
Hoechst
200 µm
Infected (GFP+)
Not infected (GFP-)
C
ViResNet architecture
3x3 maxpool, stride 2
softmax
7x7, 64, stride 2
1x1, 64
1x1, 64
1x1, 256
global average pool
Head model
D
Training quality: Operating characteristics
ViResNet
Decision tree
SVM
k-NN
True positive rate
False positive rate
HSV-1
AdV-C2
E
Predicting infection for virus not included in the training set
Input
Nuclear DNA signal
Prediction
in silico
Validation
Infection staining
AdV-C5-IX-FS2A-GFP
Hoechst
200 µm
Infected (scored)
Not inf (scored)
93% accuracy
GFP

Suppl. Fig. S2: Dataset generation pipelines and training quality of ViResNet for infection prediction (related to Fig. 3).

A) Training dataset generation pipeline for prediction of spreading and nonspreading infected nuclei, respectively.

B) Receiver operating characteristic (ROC) curves for infection prediction of trained ViResNet and multilayer perceptron. S, NS and NI denote spreader, nonspreader and not infected nuclei accordingly.

C) Average ViResNet accuracy for randomly sampled test images from different timepoints. Each datapoint is the average accuracy of test images, previously not seen by the network. Suppl. Fig. S3: Samples of prospective spreader, nonspreader and not infected nuclei at pre- and post-ablation stages (related to Fig. 5). All images are represented as Z-stacks with Nyquist sampling.

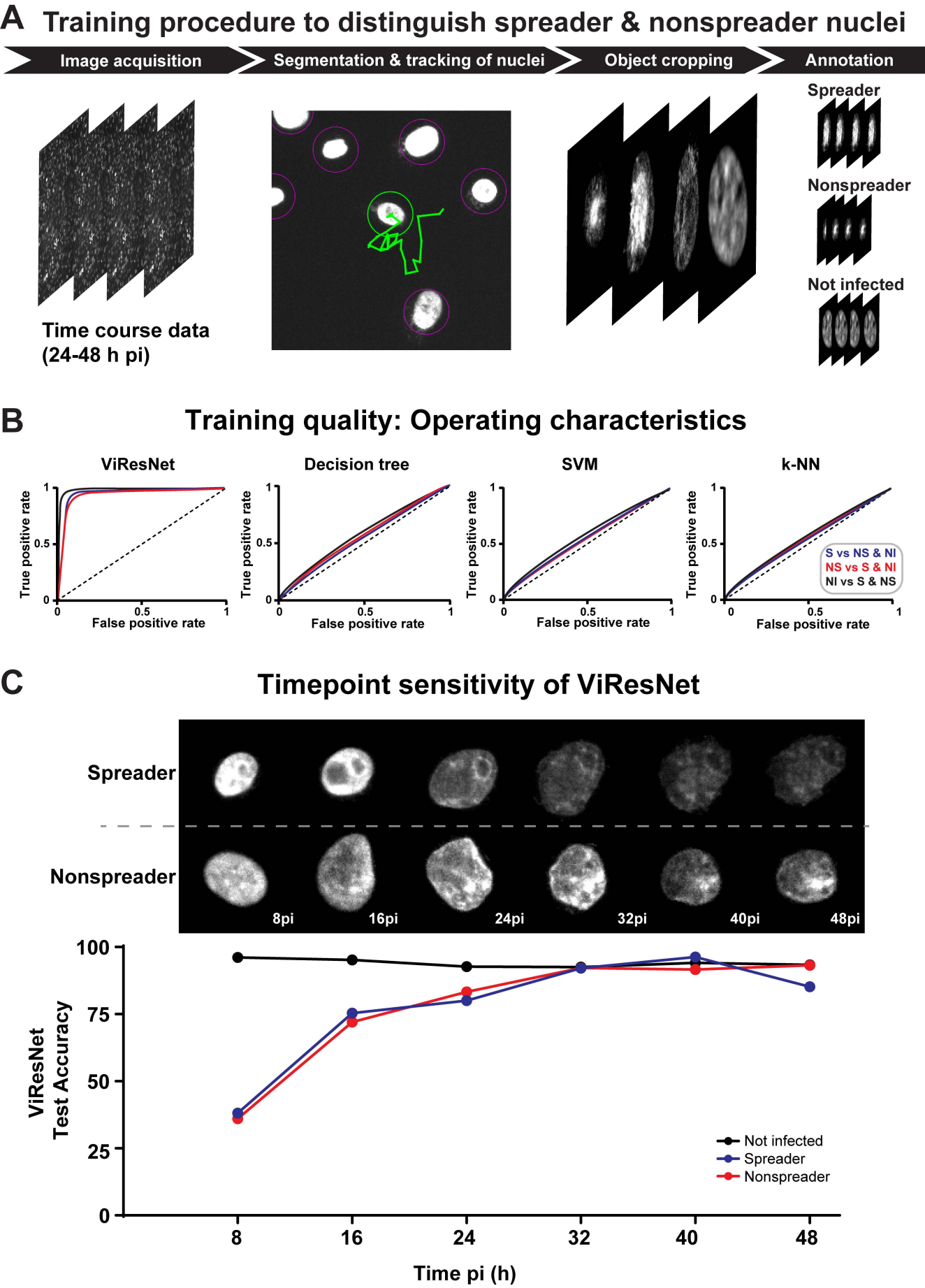
A
Training procedure to distinguish spreader & nonspreader nuclei
Image acquisition
Segmentation & tracking of nuclei
Object cropping
Annotation
Spreader
Nonspreader
Not infected
Time course data
(24-48 h pi)
B
Training quality: Operating characteristics
ViResNet
Decision tree
SVM
k-NN
True positive rate
False positive rate
S vs NS & NI
NS vs S & NI
NI vs S & NS
C
Timepoint sensitivity of ViResNet
Spreader
Nonspreader
8pi
16pi
24pi
32pi
40pi
48pi
ViResNet
Test Accuracy
Time pi (h)
Not infected
Spreader
Nonspreader

Suppl. Fig. S3: Samples of prospective spreader, nonspreader and not infected nuclei at pre- and post-ablation stages (related to Fig. 5). All images are represented as Z-stacks with Nyquist sampling.